

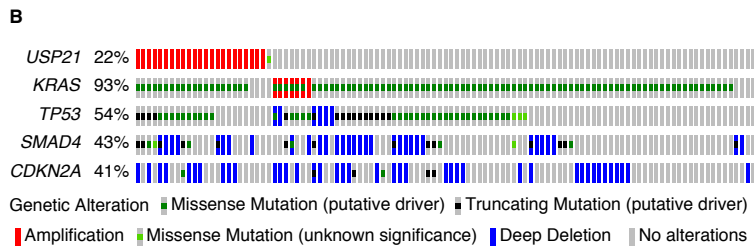
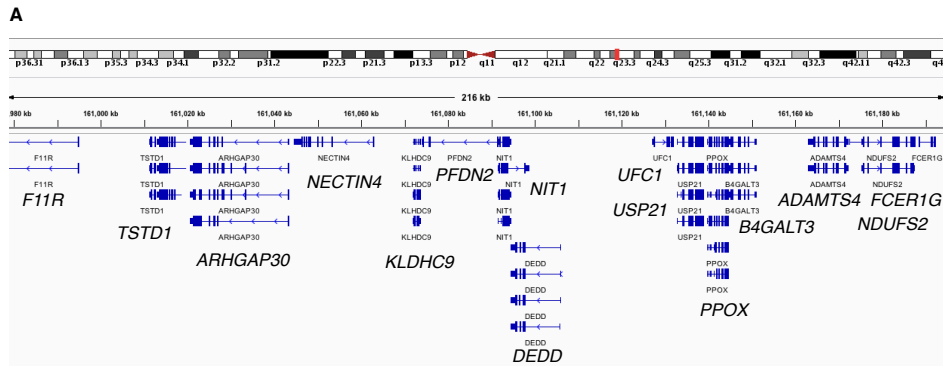
USP21 deubiquitinase promotes pancreas cancer cell stemness via Wnt pathway activation

Pingping Hou, Xingdi Ma, Qiang Zhang, Chang-Jiun Wu, Wenting Liao, Jun Li, Huamin Wang, Jun Zhao, Xin Zhou, Carolyn Guan, Jeffery Ackroyd, Shan Jiang, Jianhua Zhang, Denise J. Spring, Y. Alan Wang, and Ronald A. DePinho

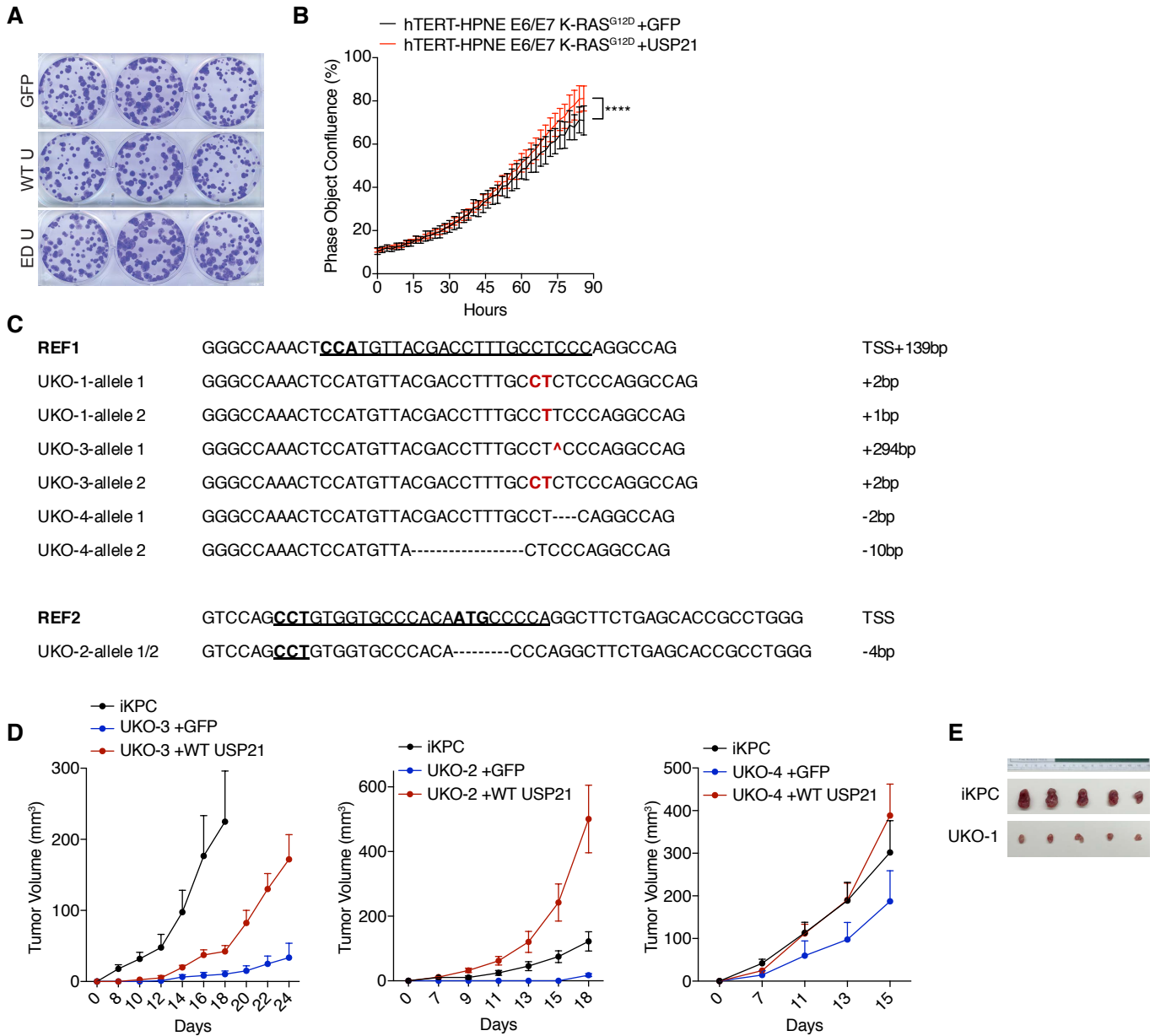
Supplemental Materials

Supplemental Figures S1-6

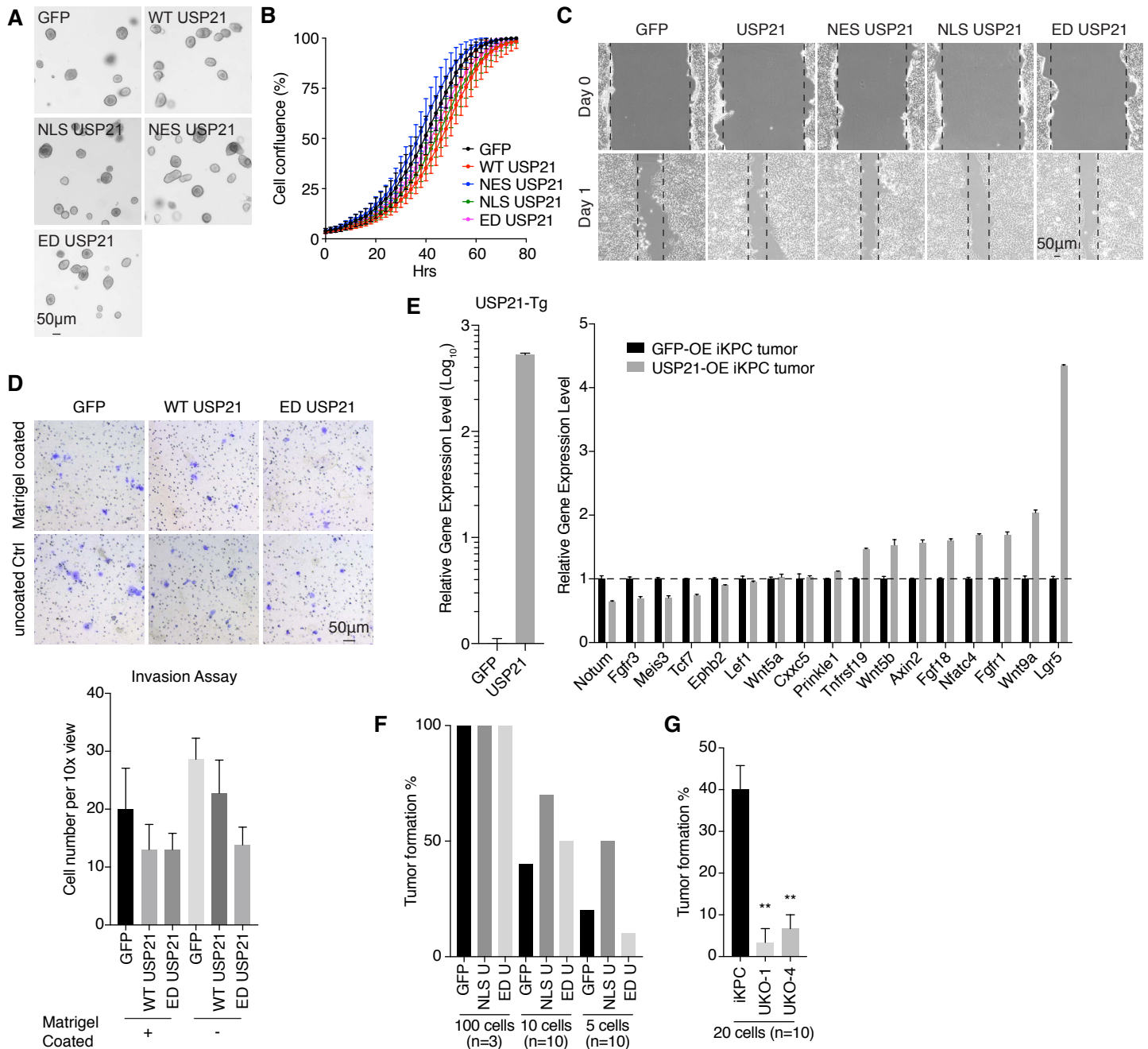
Supplemental Tables S1-2



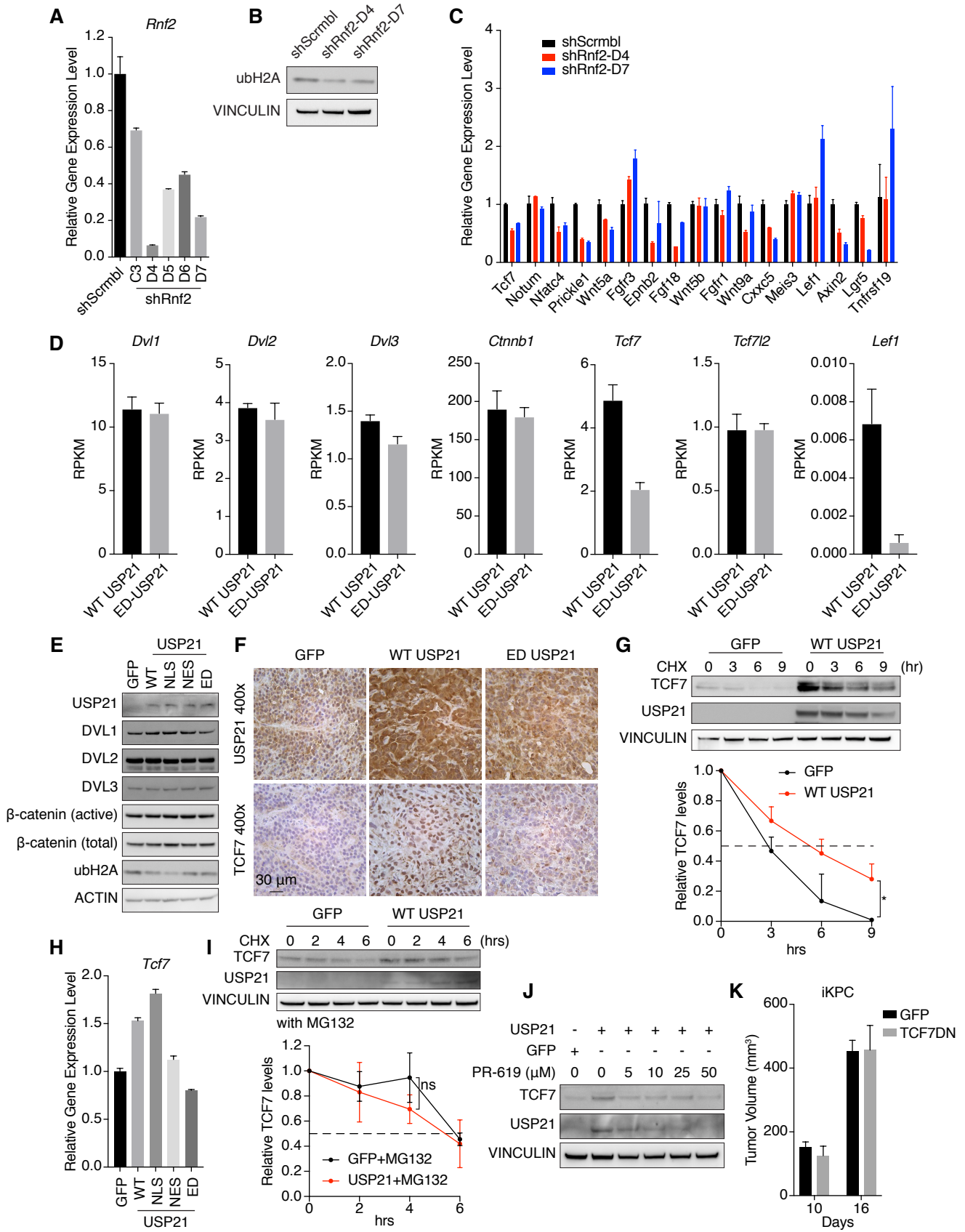
Supplemental Fig. S1. Genetic analysis of *USP21* in human PDAC data-sets. **(A)** Genes located in the minimal common region of the *USP21* amplicon. **(B)** Genetic alterations of *USP21* and other common driver genetic events in PDAC (UTSW dataset).



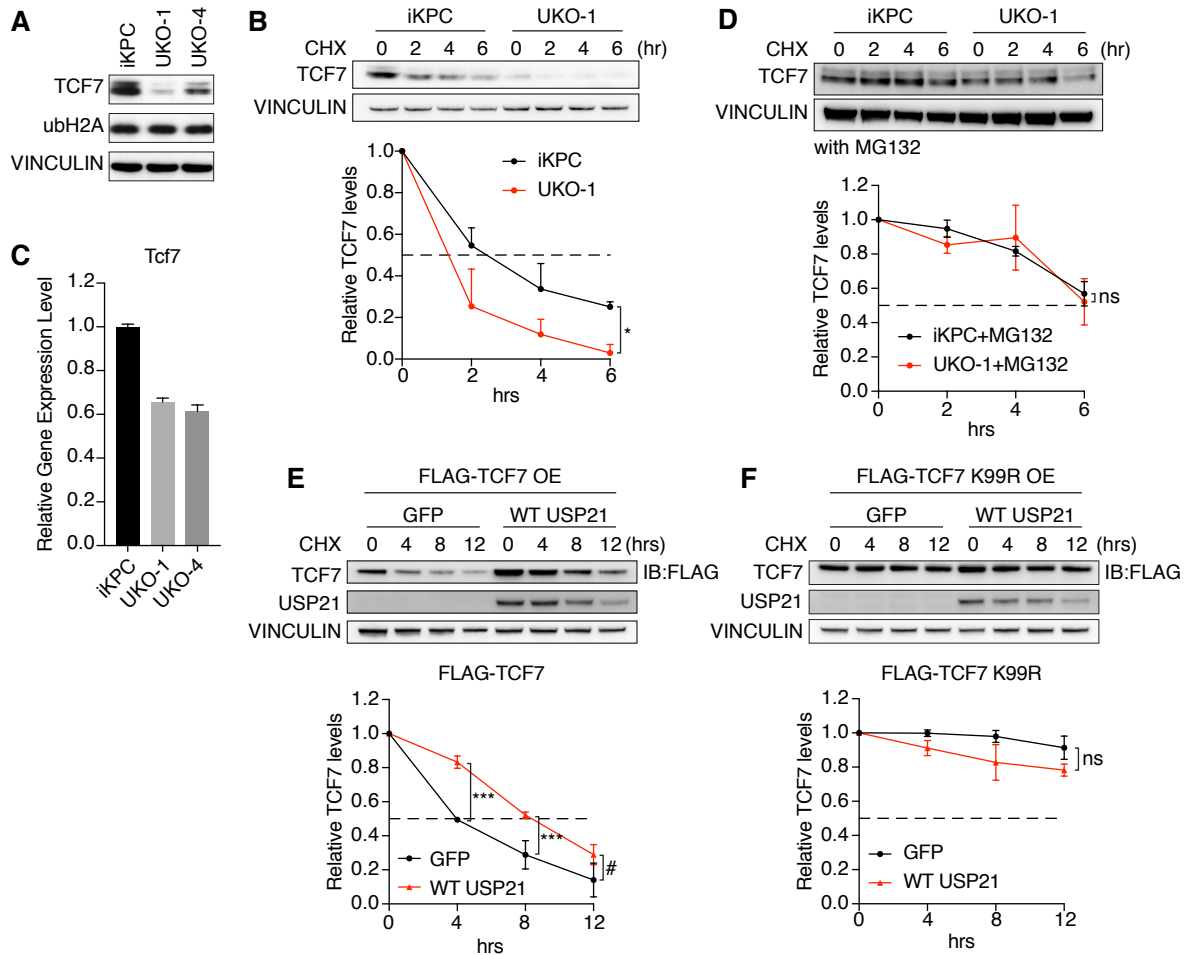
Supplemental Fig. S2. Functional analysis of USP21. (A) Colony formation assay comparing GFP, WT-USP21 (WT U) and ED-USP21 (ED U) OE iKPC cells. 500 cells per well were seeded in 6-well plates and stained with crystal violet after 1 week. (B) Cell proliferation comparing GFP and WT-USP21 OE hTERT-HPNE E6/E7-KRAS^{G12D} cells (n=6). (C) The sgRNA design to knockout *Usp21* in iKPC cells by CRISPR/Cas9. (D) Knockout of *Usp21* impaired iKPC tumor growth *in vivo* (n=5). (E) Comparison of the tumor sizes generated from iKPC cells and UKO-1 cells. For B and D, data are represented as mean ± SEM.



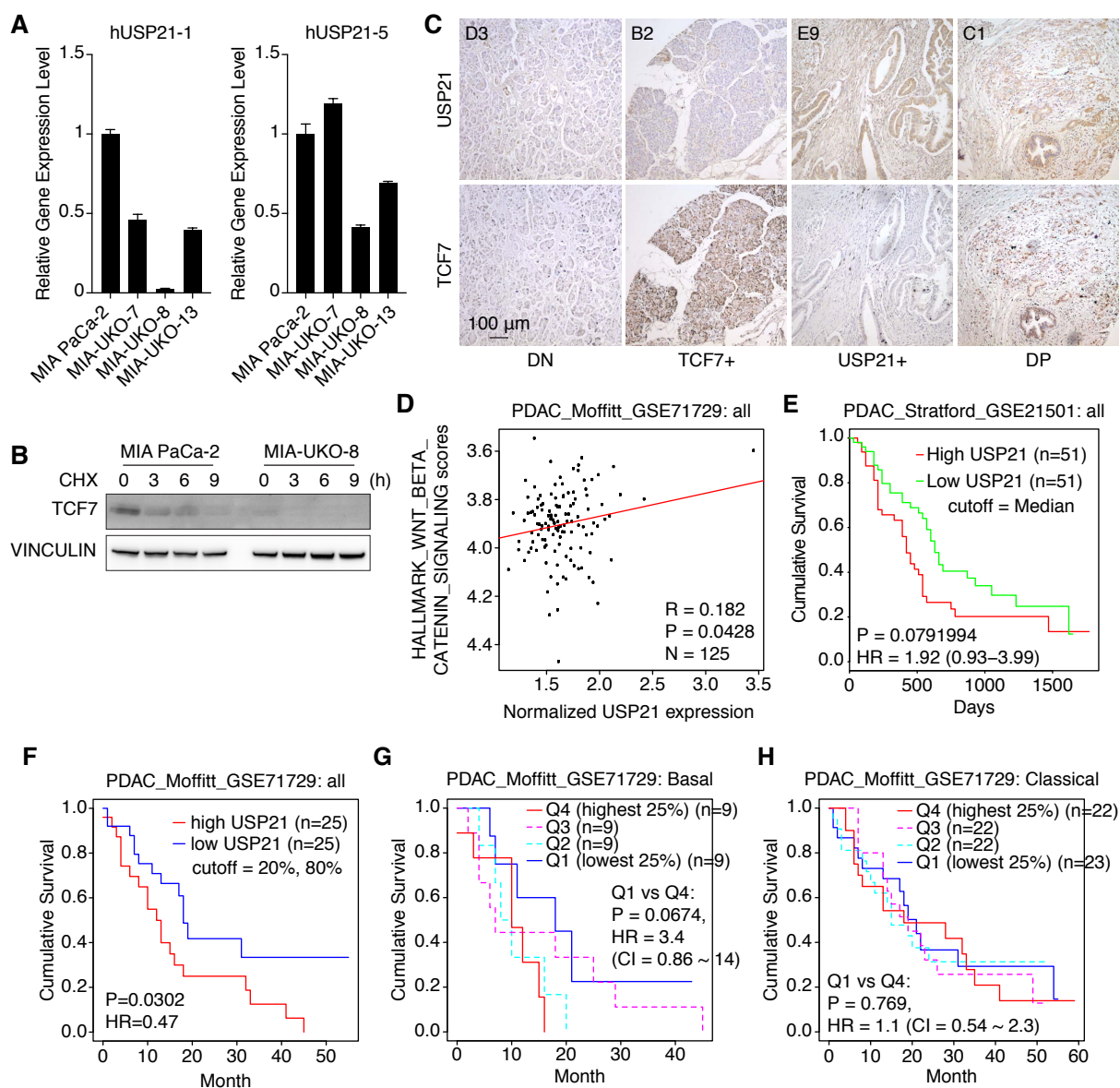
Supplemental Fig. S3. Comparison of tumorigenic functions between USP21 variants. (A-C) Spheroid colony formation in 3-D culture (A), cell proliferation assay (B) and cell migration assay (C) comparing iKPC cells overexpressing GFP and USP21 variants. (D) Cell invasion assay comparing GFP, WT- and ED-USP21 OE iKPC cells. Representative images of crystal violet staining of invaded cells and quantification were shown. (E) RT-PCR analysis of Wnt pathway genes comparing GFP and WT-USP21 OE iKPC tumors. (F) Limited dilution assay comparing GFP, NLS-USP21 (NLS U) and ED-USP21 (ED U) OE iKPC cells. 100, 10 and 5 cells were injected to compare the tumor formation rate. (G) Limited dilution assay comparing tumor formation capacity from 20 cells between *Usp21* WT and KO iKPC cells. n=3 independent experiments. For B and G, data are represented as mean ± SEM. For D and E, data are represented as mean ± SD.



Supplemental Fig. S4. USP21 activates Wnt pathway genes via TCF7 and independent of ubH2A deubiquitination. (A) Validation of *Rnf2* knockdown by shRNA (n=3). (B) Western blot analysis of ubH2A after *Rnf2* knockdown in iKPC cells. (C) RT-PCR analysis of Wnt pathway genes comparing scramble control and *Rnf2* knockdown in iKPC cells (n=3). (D) Reads Per Kilobase of transcript, per Million mapped reads (RPKM) of *Dvl1*, *Dvl2*, *Dvl3*, *Cttnb1*, *Tcf7*, *Tcf7l2* and *Lef1* extracted from RNA-seq data comparing WT- and ED-USP21 OE iKPC cells (n=4). (E) Western blot analysis of Wnt pathway proteins and ubH2A comparing iKPC cells overexpressing GFP and USP21 variants. (F) TCF7 protein levels in GFP, WT- and ED-USP21 OE iKPC tumors by IHC. (G) CHX assay of TCF7 in GFP and WT-USP21 OE iKPC cells (n=3). (H) *Tcf7* mRNA levels in iKPC cells overexpressing GFP and USP21 variants (n=3). (I) CHX assay of TCF7 in GFP and WT-USP21 OE iKPC cells with MG132 treatment (n=3). (J) Comparison of TCF7 protein levels in USP21 OE iKPC cells under DUB inhibitor PR-619 treatment at different concentrations. (K) Tumor growth comparison of GFP and TCF7DN OE iKPC cells (n=5). For A-B, and G-I, data are represented as mean \pm SD. For D and K, data are represented as mean \pm SEM.



Supplemental Fig. S5. Depletion of *Usp21* in iKPC cells destabilizes TCF7 and impairs tumor initiating capacity. (A) TCF7 and ubH2A protein levels in *Usp21* WT and KO iKPC cells by western blot analysis. (B) CHX assay of TCF7 in *Usp21* WT and KO iKPC cells (n=2). (C) *Tcf7* mRNA levels in *Usp21* WT and KO iKPC cells by RT-PCR analysis. (D) CHX assay of TCF7 in *Usp21* WT and KO iKPC cells with MG132 treatment (n=3). (E) CHX assay of exogenous FLAG-tagged TCF7 in GFP and USP21 OE 293T cells (n=3). (F) CHX assay of exogenous K99R mutated TCF7 in GFP and USP21 OE 293T cells (n=2). For B-F, data are represented as mean \pm SD.



Supplemental Fig. S6. Correlation between USP21 and TCF7 in human PDAC samples. (A) Validation of *USP21* knockout in 3 MIA PaCa-2 single cell colonies by RT-PCR using 2 different primers. (B) CHX assay of TCF7 in *USP21* WT and KO Mia PaCa-2 cells. (C) Representative images of DN, TCF7+, USP21+ and DP human TMA samples (from left to right: inflammation, normal pancreas, PDAC, PDAC, respectively). (D) Correlation analysis of Hallmark of Wnt pathway gene signature and *USP21* expression in Moffitt PDAC dataset. (E, F) Kaplan-Meier survival analysis based on *USP21* expression in Stratford PDAC dataset (E) and Moffitt PDAC dataset (F). (G, H) Kaplan-Meier survival analysis based on *USP21* expression in basal-like subtype (G) and classical subtype (H) in Moffitt PDAC dataset.

Supplementary Table 1. DNA sequence information of protein tags, sgRNA, primers and shRNA

| ID | Gene ID | Sequence | Note |
|----------------------------------|--------------|---|--------------------|
| MAPKK nuclear export signal | | CTTCAAAAAAAAACTTGAAGAACTTGAACTT | |
| SV40 nuclear localization signal | | AGCCCAAAGAAGAAGAGAAAAGTAGAA | |
| HA tag | | TACCCATACGATGTTCCAGATTACGCT | |
| FLAG tag | | GACTACAAAGACGATGACGACAAG | |
| USP21 sgRNA target | NM_001014443 | GTTAATATCCAGCCCCGAGT | sgRNA |
| hUSP21-1F | NM_001014443 | TAATATCCAGCCCCGAGTGG | shRNA validation |
| hUSP21-1R | NM_001014443 | TAACATGGGGTTTGGCCCAG | shRNA validation |
| hUSP21-5F | NM_001014443 | AGCCACCTGTTAATATCCAGCC | shRNA validation |
| hUSP21-5R | NM_001014443 | CAGAGGTCGTAACATGGGGT | shRNA validation |
| TCF7-K52R-F | XM_006532800 | CCTGGCAGAGCTCAGGTCCTCACTGGTGA | TCF7 site mutation |
| TCF7-K52R-R | XM_006532800 | TCACCAGTGAGGACCTGAGCTCTGCCAGG | TCF7 site mutation |
| TCF7-K99R-F | XM_006532800 | GAGACTTTTCCCGGACAGACTTCCAGAGTCC | TCF7 site mutation |
| TCF7-K99R-R | XM_006532800 | GGGACTCTGGAAGTCTGTCCGGGAAAAGTCTC | TCF7 site mutation |
| TCF7-K277R-F | XM_006532800 | GCCCTCCTCAGGGAGGCAGGAGCTG | TCF7 site mutation |
| TCF7-K277R-R | XM_006532800 | CAGCTCCTGCCTCCCTGAGGAGGGC | TCF7 site mutation |
| TCF7-K406R-F | XM_006532800 | CGGTACTTACCCGGAGAGGGCCGCTGC | TCF7 site mutation |
| TCF7-K406R-R | XM_006532800 | GCAGCGGCCCTCTCCGGGTAAGTACCG | TCF7 site mutation |
| shRnf2-D4 | NM_011277 | CCGGTGAGAAGCAGTACACCATTTACTCGA GTAAATGGTGTACTGCTTCTCATTTTTG | shRNA |
| shRnf2-D7 | NM_011277 | GTACCGGGTAATCTGTGCCATAAGATTTCT CGAGAAATCTTATGGCACAGATTACTTTTT G | shRNA |

Supplementary Table 2. Antibody information

| Antibody | Application | Vendor | Cat. # |
|-----------------------------|-------------|-------------------|------------|
| USP21 | IHC | Sigma | HPA028397 |
| USP21 | WB | Santa Cruz | sc-79305 |
| CYCLOPHILIN A | WB | CST | 2175s |
| LAMIN B | WB | CST | 13823 |
| TCF7 | WB, IHC | CST | 2203S |
| TCF7 | WB | CST | 2206S |
| TCF7L2 | WB | CST | 2269S |
| ACTIN | WB | Sigma | A2228 |
| FLAG | IP, WB | Sigma | F1804 |
| HA | IP, WB | BioLegend | 901501 |
| HA | WB | CST | 3724s |
| β -CATENIN (active) | WB | CST | 8814s |
| β -CATENIN (total) | WB | CST | 8480 |
| DVL1 | WB | Santa Cruz | sc-8025 |
| DVL2 | WB | CST | 3224s |
| DVL3 | WB | Santa Cruz | sc-8027 |
| ubH2A | WB | CST | 8240s |
| VINCULIN | WB | Sigma | V4505 |
| GFP | IHC | abcam | ab6673 |
| Ki67 | IHC | Thermo Scientific | RM-9106-S1 |
| Anti-rabbit IgG, HRP-linked | WB | CST | 7074s |

| | | | |
|----------------------------|----|--------|---------|
| Anti-mouse IgG, HRP-linked | WB | CST | 7076s |
| Rabbit anti-Goat IgG (H+L) | WB | Thermo | 61-1620 |